



# Radiation exchange between persons and surfaces for building energy simulations



Mette Havgaard Vorre<sup>a,\*</sup>, Rasmus Lund Jensen<sup>b</sup>, Jérôme Le Dréau<sup>b</sup>

<sup>a</sup> Energy and Environment, Danish Building Research Institute, Aalborg University Copenhagen, A. C. Meyers Vaenge 15, 2450 Copenhagen SV, Denmark

<sup>b</sup> Department of Civil Engineering, Aalborg University, Sofiendalsvej 9-11, 9200 Aalborg SV, Denmark

## ARTICLE INFO

### Article history:

Received 9 February 2015

Received in revised form 1 May 2015

Accepted 2 May 2015

Available online 12 May 2015

### Keywords:

Thermal comfort  
Mean radiant temperature  
Radiant asymmetry  
Obstacles  
View factor  
Non-rectangular surfaces  
Fanger  
PPD  
Long-wave radiation

## ABSTRACT

Thermal radiation within buildings is a significant component of thermal comfort. Typically the methods applied for calculating view factors between a person and its building surfaces requires great computational time. This research developed a view factor calculation method suitable for building energy simulations. The method calculates view factors by numerical integration of projected area factor. Over time the projected area factor of a person has been simplified by geometrical shapes. These shapes were compared with more complex equations on precision and calculation time. The same was done for the resulting view factors, where the results were compared with view factors found by ray tracing. While geometrical simplifications of the human body gave the fastest calculations, the complex equations gave the most accurate results. Non-rectangular surfaces and obstacles were treated by comparing intersection points with the edges of the surface, making the method applicable to rooms with complex geometry. The method for calculating view factors is robust and applicable to building energy simulation tools. Calculation time can be long depending on the complexity of geometry, grid-size and the choice of method for the projected area factor, but view factor calculations are done only once for a whole year simulation.

© 2015 Elsevier B.V. All rights reserved.

## 1. Introduction

Thermal radiation accounts for a substantial part of thermal comfort, and knowledge on radiation is therefore vital when simulating thermal comfort in buildings. To comply with legislation, architects and engineers work to optimise the building design in order to obtain lower energy consumption. Thermal comfort is often ensured by constraining variations in operative temperature in the energy optimisation process; but better measures would be predicted mean vote, PMV, or predicted percentage dissatisfied, PPD, and percentage dissatisfied, PD, calculated in a grid, to cover differences in the room. The overall goal is to be able to optimise the thermal comfort of the occupants in parallel with the buildings' energy consumption and the major objective is to describe a method for calculating view factors between persons and surfaces in a room for use in calculations of mean radiant temperature and radiant asymmetry.

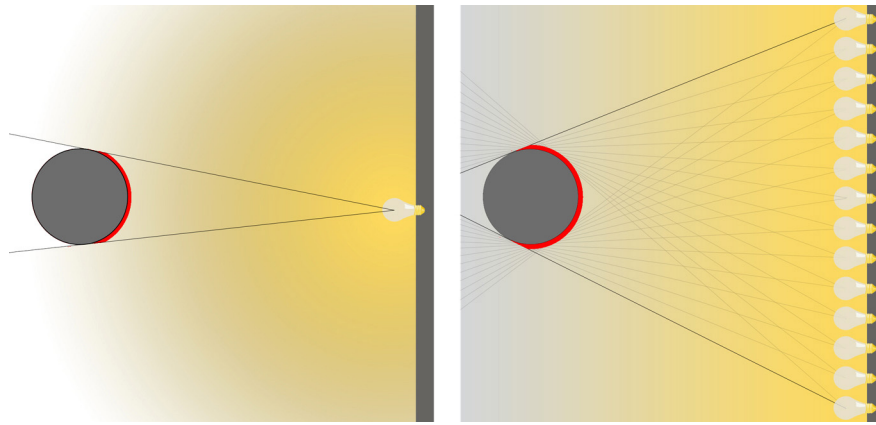
By improving the calculation of thermal comfort in building energy simulation programmes, it is possible to see the consequences on the thermal comfort when changing the building design, not just as an average in a room but on a number of different points, taking more aspects into consideration than the operative temperature. It is especially important in buildings with a complex geometry, where mean radiant temperature and radiant asymmetry varies in the room and an area-weighted mean of surface temperatures is far from accurate.

Global thermal comfort is calculated as the energy balance of the whole body, affected by 6 parameters: air temperature, mean radiant temperature, air velocity, relative humidity, clothing level and activity level [1]. Local thermal discomfort can be caused by draught, temperature gradients, asymmetric thermal radiation and cool/warm floors [2,3].

Previous work by the authors describe ways to improve the simulation of clothing level [4] and air velocity and draught risk [5] for use in building energy simulation tools.

The objective of this paper was to present a methodology for calculating thermal radiant impact on a person for better simulation of thermal comfort in building energy simulation tools. The method calculates view factors by integration of the projected area

\* Corresponding author. Tel.: +45 23 60 55 67.  
E-mail address: [mhv@sbi.aau.dk](mailto:mhv@sbi.aau.dk) (M.H. Vorre).



**Fig. 1.** To the left the projected area factor illustrated by the part of the body illuminated by a single light bulb. To the right the view factor to a wall illustrated by the part of the body illuminated by a wall of light bulbs.

factor over the surfaces and can be used for any plane surface, taking account of obstructions in the room. The method also applies for view factors for calculating radiant asymmetry. The same basic method is used for calculations between surfaces and between surfaces and a person.

For view factors involving a person, different methods and simplifications for calculating the projected area factor are compared, and the calculated view factors are compared with other methods. The comparison is made on both results and calculation time.

## 2. Theory

For the calculation of thermal comfort by using PMV or PPD and PD caused by radiant asymmetry, knowledge of the mean radiant temperature and radiant asymmetry are needed [1,3]. Mean radiant temperature is defined as that uniform temperature of a black enclosure which would result in the same heat loss by radiation as the actual enclosure under study. The definition covers both short wave radiation from the sun or a high-intensity radiant heater and long-wave radiation by emission from surfaces. This paper is focused on the latter while the impact on thermal comfort from short-wave radiation is treated by e.g. Karlsen [6]. Radiant asymmetry is defined as the difference in mean radiant temperature for each side of a small horizontal or vertical plate at the person's position in the room [7].

For comparing scenarios, the mean radiant temperature is an expression that is easier to relate to than a number of different temperatures of the surfaces.

The mean radiant temperature at a specific location is found by calculating the heat transfer through radiation in the actual enclosure. The radiant energy exchange between a person and a surrounding surface is calculated as between any two objects:

$$q_{1 \rightarrow 2} = \varepsilon \cdot \sigma_s \cdot F_{1 \rightarrow 2} \cdot A_1 \cdot (T_1^4 - T_2^4) = -q_{2 \rightarrow 1} \quad (1)$$

where  $q_{1 \rightarrow 2}$  is the heat flow by radiation from object 1 to object 2 in W,  $\varepsilon$  is the multiple of the emissivities of the objects,  $\sigma_s = 5.67 \cdot 10^{-8} \text{ W/m}^2 \text{ K}^4$  is the Stefan–Boltzmann constant,  $F_{1 \rightarrow 2}$  is the radiation view factor or angle factor from object 1 to object 2 (how big an area does object 2 cover compared with the whole area that object 1 radiates to),  $A_1$  is the effective radiation area of object 1 in  $\text{m}^2$ ,  $T_1$  is the surface temperature of object 1 in K,  $T_2$  is the surface temperature of object 2 in K,  $q_{2 \rightarrow 1}$  is the heat flow by radiation from object 2 to object 1 in W.

Eq. (1) is only valid if reflection can be disregarded; which is only a reasonable assumption when the emission of the surfaces is close to the emission of a black body, where all radiation is absorbed and

none is transmitted nor reflected. This is the case for many building materials and items of clothing, though glass is an exception as its emissivity can be very low, also for long-wave radiation.

To calculate the radiant exchange to a person, we need to know the surface temperature of the person and the surrounding surfaces, their areas, emissivities and the view factors between them.

The highest view factor is found when a surface surrounds a person, as the view factor of the surface is then equal to 1, as is the case for a sphere. The view factor is calculated from the projected area factor, and the projected area factor describes how much of an object is illuminated from a given point, as illustrated by the single light bulb in Fig. 1.

The view factor describes how much of the object is illuminated from a whole wall of light bulbs and can be found by integrating the projected area factor for each light bulb over the entire wall as illustrated to the right in Fig. 1.

For a person in a room, the sum of view factors to all surfaces equals 1.

The projected area of a person can be illustrated by his silhouette and depends on the view point to the person. The view point is described by the azimuth angle,  $\alpha$ , and the altitude,  $\beta$ , as illustrated in Fig. 2.

The effective radiation area of a person is the area that emits and receives radiation from the surroundings. This area is smaller than the total skin area of the body, as parts of the body do not exchange radiation with the surroundings, e.g. between the toes or under the arms.

### 2.1. A historical view of view factors involving persons

Interest in the view factors between a person and surrounding surfaces arose in the late 1960s with HVAC systems and Fanger's studies on thermal comfort [1]. Before then, studies on thermal radiation to persons were mostly done to calculate the impact on persons from direct solar radiation, because the military needed knowledge about the effect of the sun on soldiers [8]. The first studies in the field were therefore not with the aim of describing view factors but merely the projected area factor of a person from different angles.

In the 1930s, James D. Hardy and Eugene F. DuBois used a wrapping method to determine the effective radiation area of a person. A person was wrapped in paper like an Egyptian mummy, and the surface area was measured by rubber-coating the paper, a technique similar to the one used to measure the total area of the human skin also known as the DuBois area. The effective radiation area was found to be 78.3% and 78.4% of the total skin area for the two persons they measured [9].

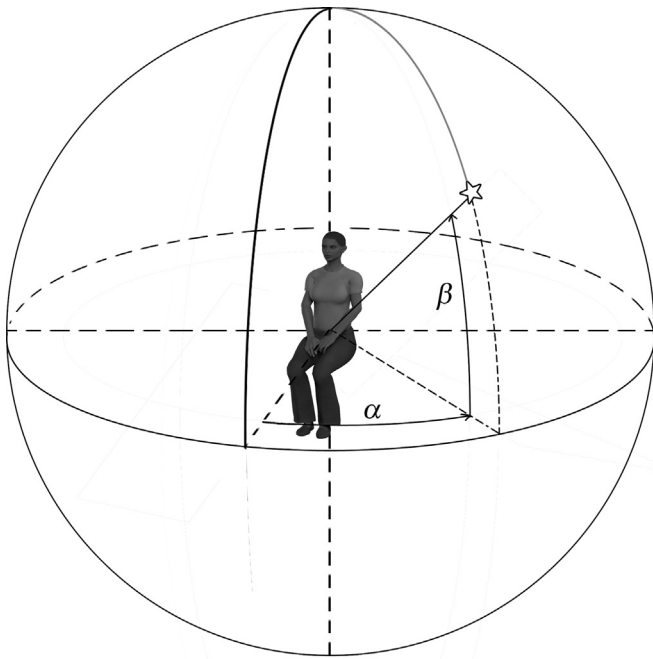


Fig. 2. The azimuth angle  $\alpha$  and the altitude  $\beta$ .

In 1952, Guibert and Taylor used photographs to determine projected areas and the total effective radiation area. Photos were taken in a half sphere, with the person in a standing and a sitting position. The pictures were taken from a distance of 12 m and treated as though taken from an infinite distance, as would be the case with radiation from the sun [10].

For calculating the projected area factor, a sphere represented a seated person and a cylinder represented a standing person. The relation between height and radius of the cylinder was found from observations [11].

As the sun was the challenge, the sun was also used in the research, and the solar angles and shadows cast were measured for a standing person facing the sun and with the person turned sideways to the sun [12].

In 1966, the photographic method was used by Underwood and Ward on standing men and women. The pictures were taken from different azimuth and altitude, though with irregular steps due to their test fixture. The photos of 25 men and 25 women were taken from a distance of 4.57 m. Underwood and Ward suggested an oval cylinder to represent a standing person in the calculations of projected area factors [13].

The photographic method and test setup of Underwood and Ward were adopted by Fanger, who in his doctoral thesis described experiments involving 10 male and 10 female test persons from northern Europe. All subjects were photographed from 78 different angles with steps of 15 degrees. Photos were taken for both a standing and a seated position. Fanger presented his results for the projected area factor as diagrams in order to get closer to the actual geometry of the human body. He supplemented with diagrams for the view factor between person and surfaces in an orthogonal room [1,14].

Discomfort caused by asymmetric thermal radiation was investigated in a climate chamber where the surface temperatures could be regulated independently for the two half-parts of the room, for a suspended ceiling or other part surfaces. In the experiments view factors between surfaces and persons were found by use of Fanger's diagrams and in 1980 the term radiant temperature asymmetry is introduced. Radiant temperature asymmetry is defined as the difference in plane radiant temperature for a small plane element

and is probably introduced in order to be able to make a direct measurement [2,3,7].

Diagrams for reading view factors to inclined surfaces were made in 1988 by use of cubic spline on Fanger's results for the projected area factor [15].

In 1990, Horikoshi et al. [16] made similar experiments as Fanger, but using an orthographic projection camera, where the parts of the person close to the camera are bigger than those further from the camera. This is in contrast to the earlier work, where an effort was put into measuring the projected area as seen from infinity. As surfaces and especially the floor are not infinitely far away, they argue that this method is more accurate especially when considering the heat exchange to floors with heating and in relatively small rooms. The results of Horikoshi et al. are presented as diagrams for reading view factors.

In the beginning of the 1990s, the computer era affected the world of thermal radiation calculation and Fanger's diagrams for reading both the projected area factor and the view factor in orthogonal rooms are put into algorithms. Just like with the principle in Fanger's diagrams for view factors, it is still necessary to divide all surfaces according to the centre of the person and categorise the divisions in front or behind, above or below the centre, on the side, vertical or horizontal [17,18].

In 2000, algorithms for view factors to inclined surfaces were added [19].

In the beginning of the new millennium, a study similar to Fanger's was made in Italy on Italian subjects. The study involved more subjects and smaller angle steps, since digital photos and computer software measure the projected area of the persons in the photos much quicker than the manual measures taken 40 years earlier. The results showed fair agreements with the projected area factors for standing persons found by Fanger, but for seated persons the differences were significant [20].

Apart from these methods, CFD programmes and computer games use ray tracing for calculating radiation very precisely. Ray tracing has a longer calculation time and demands more input than the other methods.

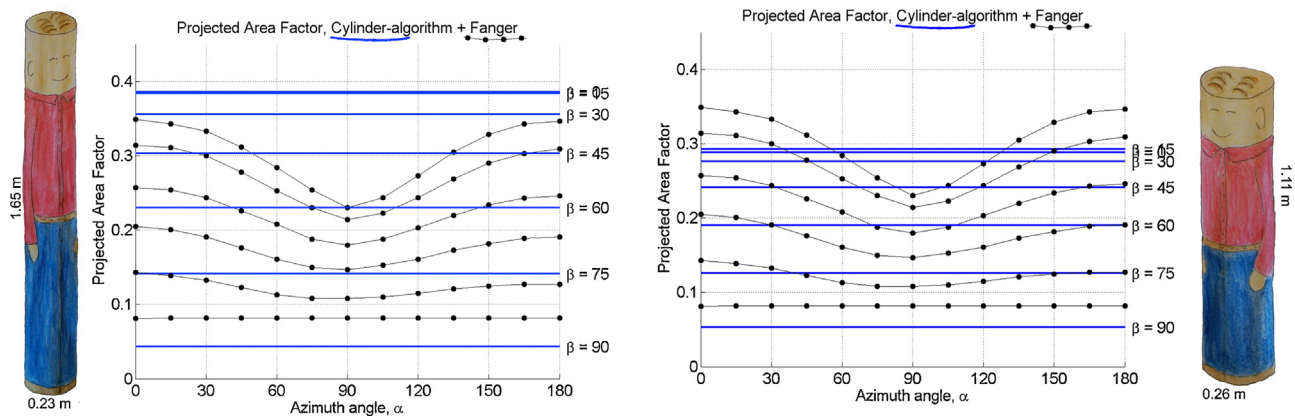
This paper suggests using numerical integration for calculation of view factors. The method was chosen because it is applicable for both person-to-surface calculations and surface-to-surface calculations. The method implies knowledge of the projected area factor of a person, or surface, as a function of the angle that the person is viewed from.

The method can also be used to compute radiant temperature asymmetry, by calculating view factors for each side of a small horizontal and a small vertical plate. The correlations between radiant asymmetry and thermal comfort are described for the small plates, though during the studies the actual view factors to the heated or cooled surfaces were also calculated. By calculating view factors for a person, while keeping track of azimuth and altitude angles, it is possible to also compute thermal radiant asymmetry for an actual person, and the results were compared to the results using small plates.

## 2.2. Projected area factor of a person—comparison of calculation methods

Over time the projected area of a person was simplified to geometrical shapes for easier use in calculations, e.g. spheres and cylinders. In this study, numerical integration is suggested for calculating view factors, and it is therefore interesting to compare the geometrical simplifications for calculation of the projected area factor to more complex algorithms on both precision and calculation time.

Comparisons were made for both standing and seated persons. The projected area factor of a seated person was calculated



**Fig. 3.** Projected area factors of a standing person, calculated by using a cylinder as suggested by Taylor [11] and optimised according to Fanger's results (thick line) compared with the results of Fanger's measurements indicated by the thin line with dots.

assuming a sphere, a cube and a box. A standing person was simplified to a cylinder and an oval cylinder. As more complex equations, the results by Rizzo et al. [17] were used. Their equations are derived from original data provided by Fanger. Unfortunately, it was not possible to obtain access to the data found in the Italian experiments [20], and the calculated values are therefore only compared with the data points from Fanger's experiments.

Only the results for standing persons are shown here. The equations for seated persons are used in the later comparison of calculated view factors.

The simplest suggestion of a standing person is a cylinder. In Fig. 3, the cylinder is compared with the results by Fanger. On the left, the cylinder is 1.65 m high and has a radius of 0.23 m as found by Taylor [11] and on the right, the cylinder was optimised by the least square error compared with Fanger's data, height 1.11 m and radius 0.26 m.

A cylinder is axisymmetric and the projected area does therefore not vary with the azimuth angle; on the other hand it does have quite an identical behaviour for the altitude.

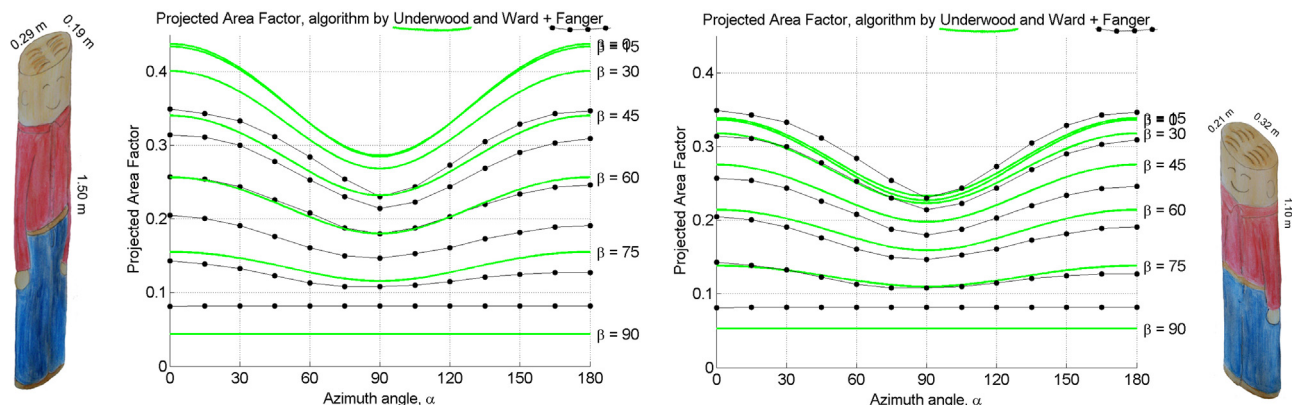
An oval cylinder of 1.5 m in height, a large radius of 0.29 m and a small radius of 0.19 m was suggested by Underwood and Ward [13]. In Fig. 4, the projected area factor of the original oval cylinder is compared with data points from Fanger on the left and on the right an optimised cylinder is compared, height 1.1 m, large radius 0.32 m and small radius 0.21 m.

The oval cylinder has many similarities with Fanger's results and depicts both the variations in azimuth and altitude.

The last method for calculating the projected area factor in the comparison is the algorithm derived by Rizzo et al. [17] on the basis of Fanger's results. The algorithm is a double variable polynomial where the azimuth angle is of degree 4 and altitude is of degree 3. The algorithm is only valid for azimuth angles between 0° and 180° and for the altitude between 0° and 90°. In Fig. 5 the algorithm is compared to the results by Fanger.

Of the three calculation methods (cylinder, oval cylinder and algorithm) the best fit is found by using the algorithm derived from Fanger's data, as shown in Fig. 5, though the algorithm shows less similarities at the front and back of the person (azimuth angle close to 0° and 180°) especially at low altitudes. The differences close to the limits of the valid range is due to the nature of the developed polynomial, as can be seen when plotting values outside the valid ranges, shown on the right side in Fig. 5.

The calculation time is the cost of achieving the higher precision by using the algorithm. While the oval cylinder is only a little slower than the simple cylinder, the algorithm's calculation time is approximately 4 times that of the cylinders. For the calculation of view factors where a high number of calculations are needed when using the integration method. The calculation time may end up being an issue, though for building energy simulation tools the calculation of angle factors are only done once for every position of the person, not at every time step.



**Fig. 4.** Projected area factors of a standing person, calculated by using an oval cylinder as suggested by Underwood and Ward [13] and an optimised oval cylinder (thick line) compared with the results of Fanger's measurements indicated by the thin line with dots.

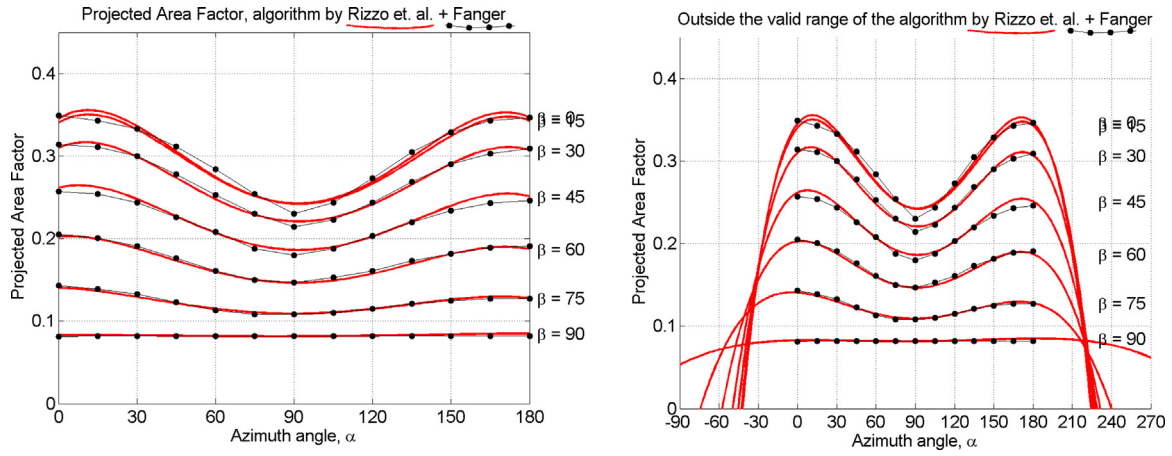


Fig. 5. Comparison of the projected area factor for a standing person as measured by Fanger (thin line with dots) and calculated using of the algorithm found by Rizzo et al. [17] (thick line). To the right is shown the behaviour of the algorithm outside the valid range.

### 3. From projected area factor to view factor for a person

In this section, a methodology is described for calculating the view factor between a person and a plane surface of any geometry, the method can also be used between two surfaces and when other surfaces obstruct the radiation.

A person receives and emits heat by radiation. If a person is placed in a sphere, all radiation from that person will hit the sphere, while not all of the radiation from the sphere will hit the person, as most of it will instead hit the sphere itself.

If the radiation is diffuse, then:

$$A_{\text{Person}} \cdot F_{\text{Person-Sphere}} = A_{\text{Sphere}} \cdot F_{\text{Sphere-Person}} \quad (2)$$

where  $A_{\text{person}}$  is the effective radiation area of a person in  $\text{m}^2$ ,  $F_{\text{Person-Sphere}}$  is the view factor from the person to the sphere (how much of the radiation leaving the person reaches the sphere),  $A_{\text{Sphere}} = 4 \cdot \pi \cdot r^2$  is the surface area of the sphere in  $\text{m}^2$ ,  $F_{\text{Sphere-Person}}$  is the view factor from the sphere to the person (how much of the radiation leaving the sphere reaches the person),  $r$  is the radius of the sphere in m.

As all radiation leaving the persons effective radiation area reaches the sphere, the view factor from the person to the sphere is known:  $F_{\text{Person-Sphere}} = 1$ , and Eq. (2) can then be written as:

$$A_{\text{Person}} = A_{\text{Sphere}} \cdot F_{\text{Sphere-Person}} \quad (3)$$

The view factor from the sphere to the person cannot be calculated directly. It has to be integrated over the surface of the sphere.

If looking at the radiation from the small area  $dA_{\text{sphere}}$  to the person, then  $dA_{\text{sphere}}$  radiates diffusely in a sphere. This radiation-sphere reaches the person at a distance equivalent to the radius,  $r$ , of the sphere, as illustrated in Fig. 6. The view factor from  $dA_{\text{sphere}}$  to the person is therefore the projected area of the person,  $A_{\text{projected}}$ , as seen from  $dA_{\text{sphere}}$  compared with the total area of the radiation-sphere with the radius  $r$  cut off by the sphere surrounding the person, which also has the radius  $r$ . The surface area of a sphere cut off by another sphere with equal radius is  $1/4$  of the total surface area of the sphere. The view factor is then given by:

$$F_{dA_{\text{sphere-Person}}} = \frac{A_{\text{projected}}}{(1/4) \cdot 4 \cdot \pi \cdot r^2} = \frac{A_{\text{projected}}}{\pi \cdot r^2} \quad (4)$$

where  $F_{dA_{\text{sphere-Person}}}$  is the view factor from the small area  $dA_{\text{sphere}}$  to the person,  $A_{\text{projected}}$  is the person's projected area as seen from  $dA_{\text{sphere}}$  in  $\text{m}^2$ ,  $r$  is the radius of the sphere in m.

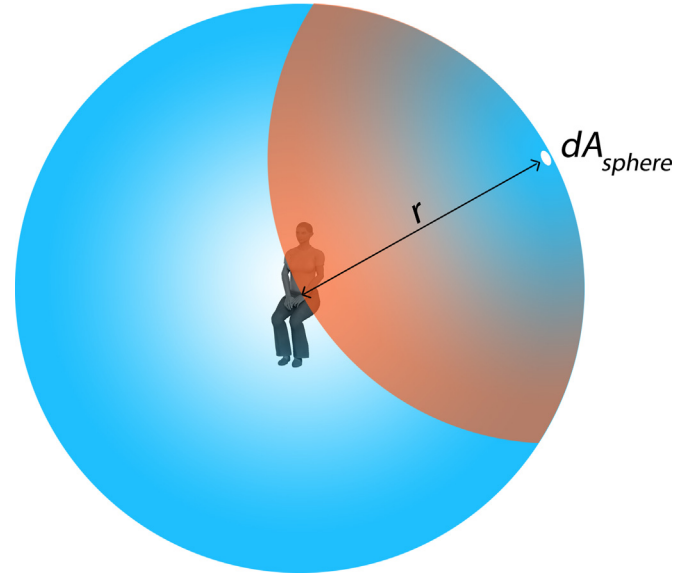


Fig. 6. A person in the middle of a sphere. The small area  $dA_{\text{sphere}}$  radiates diffusely in a sphere that is cut off by the sphere surrounding the person.

Most surfaces surrounding us are not spheres. If instead of looking at a sphere, we look at a plane rectangular surface with the area  $A$ , as shown in Fig. 7, then this area can be divided into areas so small that it is reasonable to assume that the whole area  $dA$  has the same distance to the person, and it is possible to calculate it like for the sphere.

For the small area  $dA$ , Eq. (2) can be written as:

$$A_{\text{eff}} \cdot dF_{\text{Person-dA}} = dA \cdot F_{dA-Person} \quad (5)$$

Because the person sees the small area  $dA$  under the angle  $\gamma$ , the area that the person sees is  $dA \cdot \cos(\gamma)$ , which means that the view factor from the small area  $dA$  to the person is

$$F_{dA-Person} = \frac{A_{\text{projected}}}{\pi \cdot r^2} \cdot \cos(\gamma) \quad (6)$$

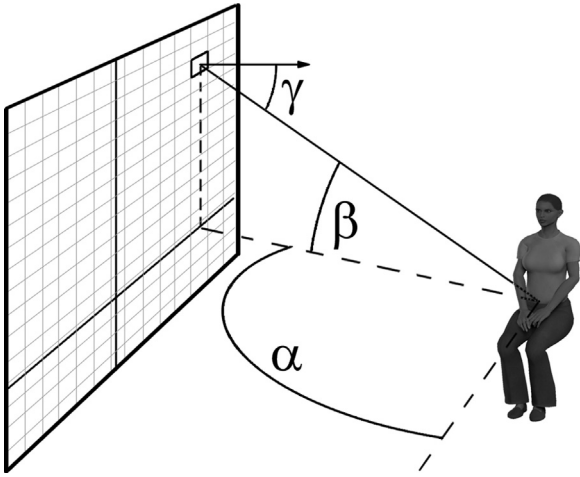


Fig. 7. Person seated beside a plane rectangular surface. The surface is divided into small areas,  $dA$ , for which the projected areas of the person are calculated.

$dF_{\text{Person}-dA}$  can then be calculated as:

$$\begin{aligned} dF_{\text{Person}-dA} &= \frac{dA \cdot F_{dA-\text{Person}}}{A_{\text{eff}}} = \frac{dA \cdot A_{\text{projected}}}{A_{\text{eff}} \cdot \pi \cdot r^2} \cdot \cos(\gamma) \\ &= \frac{A_{\text{projected}}}{A_{\text{eff}}} \cdot \frac{1}{\pi \cdot r^2} \cdot \cos(\gamma) \cdot dA \\ &= \frac{f_{\text{projected}}}{\pi \cdot r^2} \cdot \cos(\gamma) \cdot dA \end{aligned} \quad (7)$$

where  $f_{\text{projected}}$  is the projected area factor of the person, which relates the projected area of a person to the effective radiation area of the person. Like the projected area, it depends on the azimuth and altitude from where the person is viewed.

By integrating Eq. (7) over the surface, the view factor from the surface to the person can be found:

$$F_{\text{Person}-A} = \frac{1}{\pi} \int_A \frac{f_{\text{projected}}(\alpha, \beta)}{r^2} \cdot \cos(\gamma) \cdot dA \quad (8)$$

where  $r$  is the radius of the sphere with the person in the centre and reaching  $dA$  or simply the distance between the person and  $dA$ ,  $\gamma$  is the angle between the line person- $dA$  and the normal of the surface,  $\alpha$  is the azimuth angle measured from the person's sight direction to  $dA$ ,  $\beta$  is the altitude to  $dA$  from the person's centre,  $f_{\text{projected}}$  is the projected area factor.

To calculate the view factor to the entire surface, the integral in (8) must be solved, which cannot be done analytically. Instead it is solved numerically:

$$\begin{aligned} F_{\text{Person}-A} &= \frac{1}{\pi} \int_A \frac{f_{\text{projected}}(\alpha, \beta)}{r^2} \cdot \cos(\gamma) \cdot dA \\ &\approx \frac{1}{\pi} \sum_A \cdot \frac{f_{\text{projected}}(\alpha, \beta)}{r^2} \cdot \cos(\gamma) \cdot \Delta A \\ &= \frac{1}{\pi} \sum_y \left( \sum_x \cdot \frac{f_{\text{projected}}(\alpha, \beta)}{r^2} \cdot \cos(\gamma) \cdot \Delta x \right) \cdot \Delta y \end{aligned} \quad (9)$$

The Simpson method is used for the numerical integration of Eq. (9) and the procedure is described in Appendix.

View factors for calculation of radiant asymmetry are found by setting the projected area factor to zero, when the azimuth angle is to the left/right of the person or the altitude angle is above/below zero.

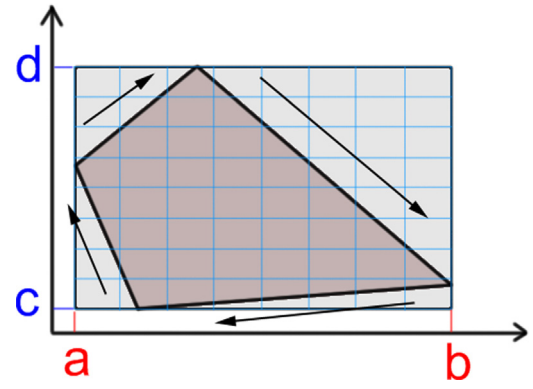


Fig. 8. Example of a non-rectangular surface with the vectors constituting the edges of the surface.

### 3.1. Complex geometries

The described method of integration over the surface is only applicable if the surface is rectangular. If it is not, the method should be supplemented with extra calculations.

For a non-rectangular surface, a rectangular surface is made that includes the whole surface, as shown in Fig. 8. The rectangular surface is then divided by a grid for the numerical integration and for each node it is checked, whether or not it is a part of the real surface.

The position of all nodes is compared with the edge vectors of the real surface. If the node lays to the right of all edge vectors, it is within the surface. If the node lies to the left of just one edge, it is outside the real surface. The method is only valid for surfaces where all corner angles are less than  $180^\circ$ . If this is not the case, the surface needs to be divided into smaller surfaces where all angles are smaller than  $180^\circ$ .

The process is quite slow, so to reduce calculation time the check for a node against edge vectors is stopped if the node is found to lie to the left of an edge, as there is then no reason to check against other edges. Furthermore, it is seen that when going perpendicularly through the rectangular grid, if one node is inside the real surface and the next is outside, then all the following nodes in that row or column will also be outside.

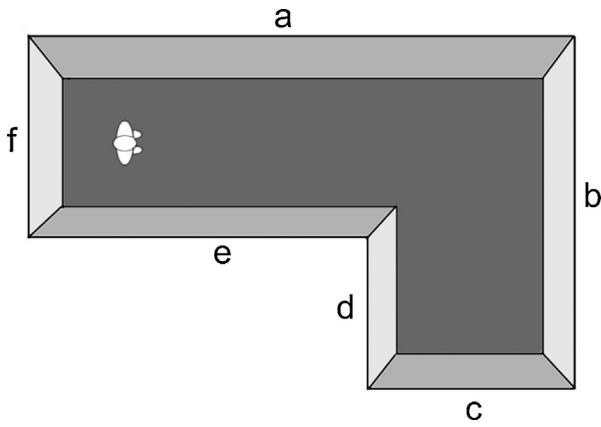
If it is found that the node is outside the real surface, the projected area factor in Eq. (9) of the subsurface is set to zero, otherwise the actual projected area factor is determined.

In the case of a room with one or more surfaces that in reality have corner angles more than  $180^\circ$ , it is important to realise that the person can actually be positioned “behind” some of the surfaces in the room. In Fig. 9, the person has a view factor of zero to surface  $d$ , because the person is positioned behind the surface.

### 3.2. Obstructions between surface and person

The method of comparing a point to the edges of the surface is also used to determine whether other surfaces are obstructing the view between a subsurface and the person.

When calculating view factors between the person and surface  $b$  in Fig. 9, the vectors between the person and each node on the surface are found. For each vector, it is checked whether the vector is blocked by another surface. If the intersection point of the vector on another surface is within the edges of the other surface, then the radiation is blocked, though only if the intersection point is between the person and the node. In Fig. 9, radiation from surface  $b$  is partly blocked by both surface  $d$  and surface  $e$ , but as soon as it is found that the vector is blocked by one surface, there is no need to check intersection points with any other surfaces.



**Fig. 9.** L-shaped room seen from above with a person. View factor between person and wall *d* equals zero. The view factor to wall *c* is also zero, as radiation between the surface and the person is blocked by surfaces *d* and *e*.

The vector between a node on surface *b* and the person can intersect with surface *f*, but the intersection point lies outside the range of the vector and is therefore irrelevant.

This is potentially a very slow process because all surfaces have to be checked, and consequently it is possible to simply disregard this step, if the room geometry yields that surfaces cannot block one another e.g. all corner angles are smaller than 180°.

Secondly, before the calculations of view factors are started, the potential obstructing surfaces are found for each surface and only these surfaces are checked. In an L-shaped room as shown in Fig. 9, walls “*d*” and “*e*” are the only walls that can block radiation. The rest of the walls will never block radiation between a person and a surface, regardless of where in the room the person is positioned.

### 3.3. View factors between surfaces

Surface temperatures in a room depend on the exchange of thermal radiation between surfaces. Consequently, view factors between surfaces are also necessary for improving the calculation of the radiant part of an occupant’s thermal comfort. It is chosen not to take the obstruction by persons into consideration.

Before the use of computers, diagrams were used to find view factors between two surfaces for a number of standard situations and even though they were indeed useful, it was also a puzzle when the building under study did not fit into these standard geometries. As radiant energy exchange is a challenge also in other industries, several geometries can be handled by use of geometric equations, but for use in building energy simulation it is difficult to make a general solution with the minimum of user interaction and knowledge in the specific field.

Georg Walton tests different integration methods on both calculation time and precision, and further describes the method of integrating along the edges of the surfaces. His method integrates over any surface with corner angles of less than 180°. Obstructions between surfaces are handled by dividing the surfaces into smaller parts based on shadow cast by the obstruction [21].

In this paper it is chosen to use the same integration method for determination of view factors between surfaces as used for determination of view factors to persons. Because of the high irregularity of the human body, the method of integrating along the edges of the surfaces is not applicable when persons are involved. In order to determine the view factor between two surfaces, area integration of both surfaces is necessary and the Simpson method is therefore used twice.

For geometries other than rectangular surfaces, an orthogonal grid is still used and a check is made to determine whether a given

point is part of the actual surface. The same method is used when other surfaces or objects obstructs parts of the radiation between two surfaces.

For radiation between any two objects the following interaction applies:

$$F_{1 \rightarrow 2} \cdot A_1 = F_{2 \rightarrow 1} \cdot A_2 \quad (10)$$

where  $F_{1 \rightarrow 2}$  is the view factor from object 1 to object 2 (how much of the radiation leaving object 1 that reaches object 2),  $A_1$  is the area of object 1,  $F_{2 \rightarrow 1}$  is the view factor from object 2 to object 1, and  $A_2$  is the area of object 2. The view factor states how much of the total radiation from one object that reaches the other object and is therefore a factor between 0 and 1.

For two surfaces the view factor from surface 1 to surface 2 can be calculated as:

$$F_{1 \rightarrow 2} = \frac{1}{A_1 \cdot \pi} \cdot \int_{A_1} \int_{A_2} \frac{\cos \gamma_1 \cdot \cos \gamma_2}{r^2} \cdot dA_1 \cdot dA_2 \quad (11)$$

where  $A_1$  is the area of surface 1,  $A_2$  is the area of surface 2,  $r$  is the distance between  $dA_1$  and  $dA_2$ ,  $\gamma_1$  is the angle between the normal to surface 1 and the line between  $dA_1$  and  $dA_2$ , and  $\gamma_2$  is the angle between the normal of to surface 2 and the line between  $dA_2$  and  $dA_1$ .

The integral is solved numerically:

$$F_{1 \rightarrow 2} = \frac{1}{A_1 \cdot \pi} \cdot \int_{A_1} \int_{A_2} \frac{\cos \gamma_1 \cdot \cos \gamma_2}{d^2} \cdot dA_2 \cdot dA_1$$

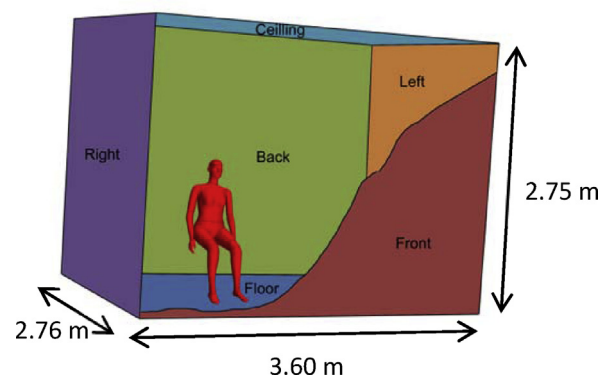
$$\approx \frac{1}{A_1 \cdot \pi} \cdot \sum_{A_1} \left( \sum_{A_2} \frac{\cos \gamma_1 \cdot \cos \gamma_2}{d^2} \cdot \Delta A_2 \right) \cdot \Delta A_1 \quad (12)$$

The numerical solution is found by using the Simpson method twice and is further described in Appendix.

## 4. Calculation example and comparison of methods

The described method was used for the calculation of view factors between a person and the surrounding surfaces in a room by using four different assumptions for calculating the projected area factor. The results were compared with the algorithm for direct calculation of view factors by Cannistraro et al. [18] and results by using ray tracing in the CFD software ANSYS CFX.

The calculations were made for a rectangular room with a seated person. The room geometry was chosen in order to be able to calculate view factors by the algorithm of Cannistraro et al. and the seated position chosen in order to compare results with a ray



**Fig. 10.** Sketch of the room used in the example with colour code for surfaces used in the diagrams.

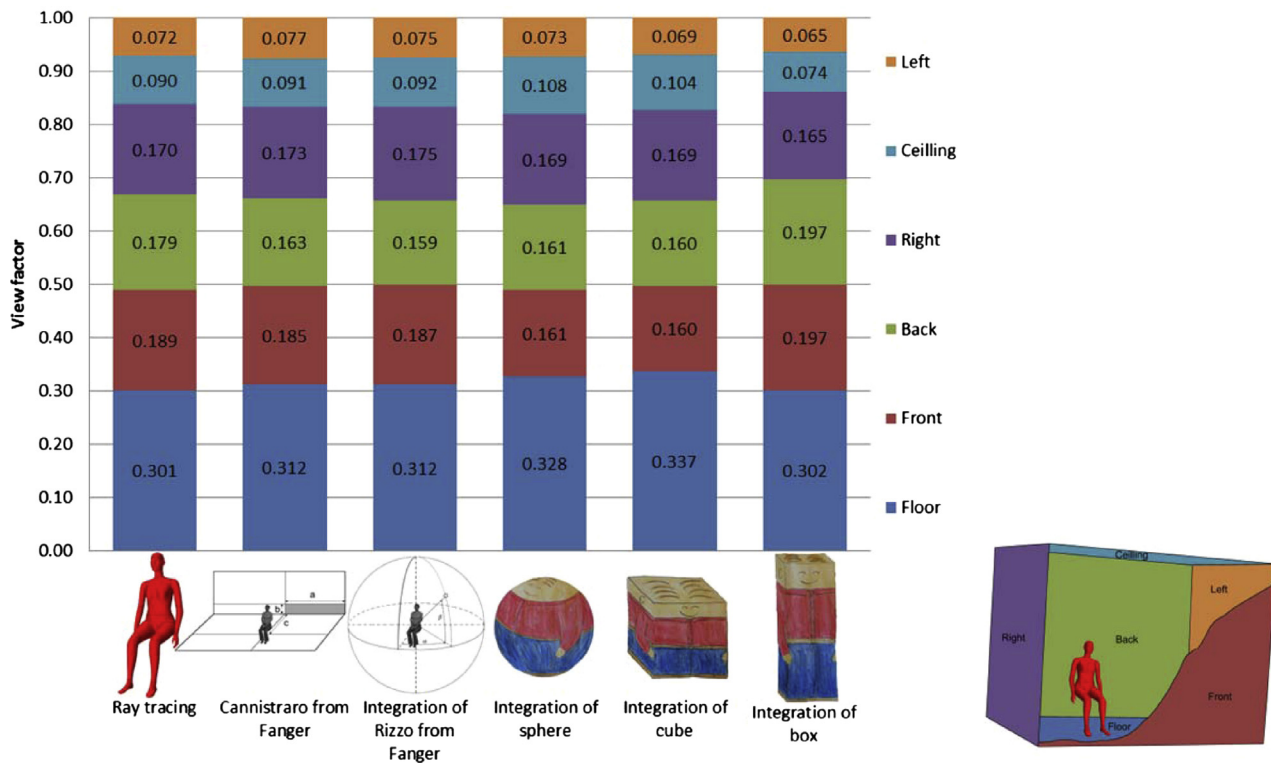


Fig. 11. View factors calculated by using six different methods.

tracing model of a person modelled by a 3D laser scan of a thermal mannequin.

The room is 3.60 m long, 2.76 m wide and 2.75 m high. The person is seated 1.2 m from the end wall and 1.38 m from the side walls, facing a side wall (Fig. 10).

In the CFD software, the view factors were found by giving all surfaces in the enclosure the same temperature and applying a higher temperature to the person. The amount of heat received by each surface was then used to calculate the view factors.

For each surface the view factor was found by numerical integration using four different methods for the calculation of the projected area factor of a seated person: the algorithm by Rizzo et al. [17] based on Fanger's results, a sphere, a cube and a box. The dimensions of the box were optimised for the best fit with Fanger's data.

The view factors were adjusted to sum up to 1 by dividing each calculated view factor with the sum of the view factors for the whole room. The calculated view factors are shown in Fig. 11 and when comparing to ray tracing, the difference is shown in Fig. 12.

The view factors in the calculation methods based on Fanger's work were the ones getting closest to the view factors found by ray tracing. The two simplest models, the cube and the sphere, differ the most. Complete agreement is probably not possible as the precise position of the seated person in the CFD model and the subjects photographed by Fanger could very well be different.

Another significant difference between the methods is the calculation time. The calculations were made in MatLab with steps of 0.01 m for the integration methods. The longest calculation time was for the integration of the algorithm for the projected area factor derived by Rizzo from Fanger's data [17]. Only 50% of that time was used if assuming a geometrical shape, and just 1% was used for the method of direct calculation of view factors as developed by Cannistraro from Fanger's data for view factors [18].

But the example given was a very simple room. There were no inclined surfaces, the person was looking directly at a surface and everything was orthogonal. All surfaces had points correlated to the centre of the person, so no special calculations were needed.

#### 4.1. Grid size

When using a numerical integration method, the chosen grid size influences both the result and the calculation time. In the above example, a grid spacing of 0.01 m was used. If instead a grid space of 0.1 m had been used, the calculation time would be reduced from 0.64 s to 0.02 s when calculating the projected area factor for the room shown in Fig. 10 and calculating the projected area factor by the method of Rizzo et al. [17]. In Table 1, the results of using a different grid sizes are shown together with the time used for calculating view factors of all six surfaces.

For the room in shown in Fig. 10 it is seen that calculation time increases rapidly when decreasing grid size and that only little difference is found in the calculated view factors, when the grid size gets minor than 0.05 m.

By accepting slightly more uncertainty in the results, it is possible to greatly reduce the calculation time, though it is important to bear in mind that the calculation of view factors only need to be done only once for a building simulation for a whole year.

#### 4.2. Effect of calculation method on mean radiant temperature and PMV

Mean radiant temperature, PMV and PPD are affected by thermal radiation and are the measures used for assessing global thermal comfort. The investigation of methods for calculation of the projected area factor and proposal of a method for view factor calculation had the purpose of improving the accuracy in



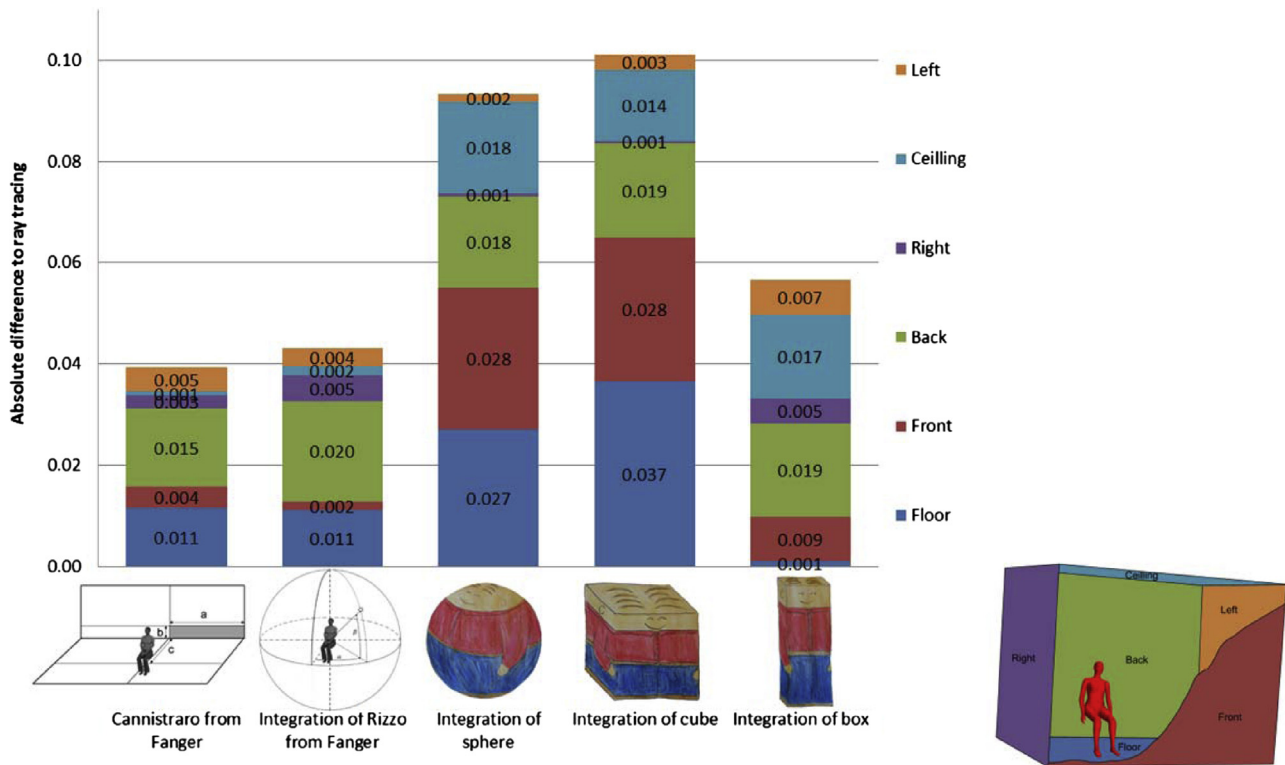


Fig. 12. Difference between view factors calculated by ray tracing and five other methods.

**Table 1**  
Calculated view factors for different grid sizes. All view factors are calculated using the method by Rizzo et al. for calculating projected area factor. The right column shows the calculation time for the room in Fig. 10.

Gridsize in m	View factors for surfaces						Calculation time in seconds
	Left	Front	Right	Back	Floor	Ceiling	
1.000	0.074	0.191	0.173	0.164	0.307	0.091	0.00
0.500	0.075	0.187	0.175	0.159	0.314	0.091	0.01
0.100	0.076	0.188	0.175	0.159	0.311	0.092	0.02
0.050	0.076	0.186	0.175	0.159	0.311	0.092	0.05
0.010	0.076	0.186	0.175	0.159	0.311	0.092	0.64
0.005	0.076	0.186	0.175	0.159	0.311	0.092	3.24
0.001	0.075	0.185	0.174	0.158	0.309	0.091	93.40

the calculation of mean radiant temperature and PMV, and it is therefore interesting to see the influence that the calculation methods has on these values.

If assuming the same emissivity for all surfaces and that reflections can be disregarded, then the mean radiant temperature can be calculated using Eq. (13):

$$T_{mr}^4 = \sum_{i=0}^n (F_{\text{person} \rightarrow \text{surface } n} \cdot T_{\text{surface } n}^4) \quad (13)$$

In the room shown in Fig. 10 all surfaces are set to have the same temperature of 22 °C, except for the wall in front of the person which is assumed to be a poorly insulated window with a surface temperature of 5 °C. Air temperature is set to 22 °C, air velocity to 0.01 m/s, clothing level to 1 clo, activity level to 1 met and relative humidity to 50%. The difference in mean radiant temperature (MRT), PMV and PPD by using the different methods are calculated and results are shown in Table 2.

In this example, integration over Rizzo is the most accurate, but it will vary depending on the error of view factors on the different

surfaces. Depending on the calculation method, the mean radiant temperature is calculated to be as low as 18.87 °C and up to 19.47 °C, giving a variation in PMV ranging from –0.68 to –0.60 and PPD ranging from 14.6% to 12.7%.


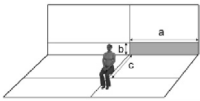
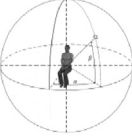



If instead the wall to the right had been the window, see Fig. 10, the two simplest methods (sphere and cube) would have been the most accurate. However, the objective was to illustrate the effect on the mean radiant temperature felt by the person.

#### 4.3. Radiant asymmetry

Radiant asymmetry can cause discomfort, both for vertical and horizontal asymmetry. The relation between the percentage of people feeling discomfort and radiant asymmetry apply for the difference in thermal radiation side-to-side for a horizontal or a vertical plate [22], though Fanger's diagrams were actually used in especially the first studies [2].

With the method described earlier in this article it is possible to calculate the radiant asymmetry for both plates and a person represented by the algorithm of Rizzo et al. by keeping track on

**Table 2**  
Results for mean radiant temperature, PMV and PPD when using different methods for calculating view factors.

						
	Ray tracing	Cannistraro	Rizzo	Sphere	Cube	Box
MRT (°C)	19.01	19.08	19.04	19.46	19.47	18.87
PMV	-0.66	-0.65	-0.66	-0.61	-0.60	-0.68
PPD	14.1	13.9	14.0	12.7	12.7	14.6

when the azimuth angle is to the right or left of the person and when the altitude angle is above or below the persons centre.

For the room in Fig. 10 the surfaces has one at a time been assumed to be a window with a surface temperature of 5 °C while the rest where kept at 22 °C. The results for radiant asymmetry at the point of the person are shown in Table 3 together with the calculated percentage of dissatisfied.

Radiant asymmetry calculated for a plate is higher than if calculating using more realistic human model. The difference between the methods is highest when the cold surface is parallel to the plate.

Using the more realistic human model in calculations of mean radiant temperatur will result in an underestimation of percentage dissatisfied.

**5. Discussion**

The described method for calculation of view factors is a robust method and can be used to explore several positions and orientations of the person in a room. The calculation time is sensitive to the choice of method for determining the projected area factor and the grid size. Both also have an effect on the accuracy of the calculated view factors. In the example, the calculation time varied by a factor 2 depending on method, while the calculated mean radiant temperature varied by 0.6 °C.



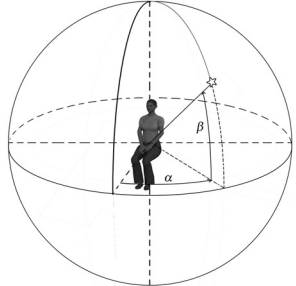
The objective of the paper was to develop a method for improving calculation of the radiant impact on occupants in building

energy simulation tools. As the calculation of view factors only has to be performed once for a given room geometry, and not at every time step in a building simulation for a whole year, the higher calculation time can be justified in order to obtain more accurate results and the method is therefore clearly applicable for building energy simulation tools also in rooms with a complex geometry.

View factors involving persons are sensitive to the method for calculating the projected area factor of the person, both in calculation time and precision. Though even with the most complex model, it is still just a model, not taking into consideration the chair and the table where a person is normally seated. And it is relevant to consider whether the error when using a simplification of a person as a sphere compared with the complex model is actually larger than the difference between the complex model and reality, where e.g. the chair blocks a substantial part of the radiation to and from the person.

The calculation of radiant asymmetry using the algorithm by Rizzo, resulted in an underestimation of percentage dissatisfied, but the results come closer to how surfaces affect a real person. Further comparison between radiation asymmetry calculated for plates and the algorithm are suggested e.g. using the results of the original studies, in order to describe the relation between percentage dissatisfied and the more realistic radiant asymmetry. The current relation simplifies the problem to what is easily measured, whereas computers and thermal mannequins make it possible to improve both measurements and calculations to better reflect reality.

**Table 3**  
Radiant asymmetry calculated by the proposed method, using a plate and the algorithm for projected area factor by Rizzo et al, and the percentage dissatisfied caused by radiant asymmetry.

							
		Vertical plate		Horizontal plate		Rizzo	
		$\Delta T_{\text{radiant}}$ (°C)	PD (%)	$\Delta T_{\text{radiant}}$ (°C)	PD (%)	$\Delta T_{\text{radiant}}$ (°C)	PD (%)
Left/right	Cold wall in front	1.2	0.2			0.9	0.2
	Cold wall to the right	8.8	2.7			5.6	0.9
	Cold wall to the left	4.2	0.6			2.4	0.3
Up/down	Cold wall in front			-2.3	0.0	-2.8	0.0
	Cold floor			14.7	37.6	10.2	20.2
	Cold ceiling			-6.1	0.1	-2.9	0.0

### 6. Conclusion

A method for calculating view factors between persons and surfaces by using Simpson integration was described and compared with ray tracing. Depending on the chosen way of calculating the projected area factor of the person, the results got close to the ones found by ray tracing, though with a much lower calculation time and a simpler setup for a user.

The method is applicable for both simple and complex rooms.

### Acknowledgements

This paper is part of a PhD study which is financially supported by the Danish Energy Research and Development Programme ELFORSK, VELUX A/S and WindowMaster A/S.

### Appendix

This appendix describes the calculation of angles used for determining projected area factors in the calculations of view factors and describes the basis in the Simpson method for numerical integration together with a quick way to build up the matrix used to weigh the results.

#### A.1. Surface to persons

For the calculation of the projected area factor, the angles  $\alpha$ ,  $\beta$  and  $\gamma$ , in Fig. 7, must be known for each small area of the surface as well as the distance,  $r$ , between the person and the small area.

The normal vector of the surface,  $\vec{n}$ , is known as well as the position,  $P$ , and the orientation,  $\vec{o}$ , of the person in the room:

$$\vec{n} = \begin{bmatrix} x_n \\ y_n \\ z_n \end{bmatrix} \quad P = \begin{bmatrix} x_p \\ y_p \\ z_p \end{bmatrix} \quad \vec{o} = \begin{bmatrix} x_o \\ y_o \\ z_o \end{bmatrix}$$

Then the angle,  $\gamma$ , between the normal vector of the surface,  $\vec{n}$ , and the vector,  $\vec{r}$ , is:

$$\cos(\gamma) = \frac{\vec{n} \cdot \vec{r}}{|\vec{n}| \cdot |\vec{r}|} = \frac{\begin{bmatrix} x_n \\ y_n \\ z_n \end{bmatrix} \cdot \begin{bmatrix} x_r \\ y_r \\ z_r \end{bmatrix}}{\sqrt{x_n^2 + y_n^2 + z_n^2} \cdot \sqrt{x_r^2 + y_r^2 + z_r^2}} \quad (14)$$

The azimuth angle,  $\alpha$ , is found in the same way, using the person's orientation,  $\vec{o}$ , and the vector,  $\vec{r}$ , though only calculated in the horizontal plane:

$$\cos(\alpha) = \frac{\vec{o}_{xy} \cdot \vec{r}_{xy}}{|\vec{o}_{xy}| \cdot |\vec{r}_{xy}|} = \frac{\begin{bmatrix} x_o \\ y_o \end{bmatrix} \cdot \begin{bmatrix} x_r \\ y_r \end{bmatrix}}{\sqrt{x_o^2 + y_o^2} \cdot \sqrt{x_r^2 + y_r^2}} \quad (15)$$

The altitude,  $\beta$ , is the angle between the vector,  $\vec{d}$ , and the projection of the vector,  $\vec{d}$ , onto the horizontal plane:

$$\cos(\beta) = \frac{\vec{r} \cdot \vec{r}_{xy}}{(|\vec{r}| \cdot |\vec{r}_{xy}|)} = \frac{\begin{bmatrix} x_r \\ y_r \\ z_r \end{bmatrix} \cdot \begin{bmatrix} x_r \\ y_r \\ 0 \end{bmatrix}}{\sqrt{x_r^2 + y_r^2 + z_r^2} \cdot \sqrt{x_r^2 + y_r^2}} \quad (16)$$

The Simpson method is used to optimise the calculation time when solving Eq. (9). The Simpson method combines the centre method with the trapeze method, where the value of a small area is calculated at the centre of the area and as a mean of the values in the corners. The method requires the number of small areas to be an even number in both directions.

The principle can be written as:

$$\int_A f(x, y) \cdot dA = \int_a^b \int_c^d f(x, y) \cdot dy \cdot dx$$

$$\approx \begin{bmatrix} f(a, c) & f(a+k, c) & f(a+2k, c) & \dots & f(b-2k, c) & f(b-k, c) & f(b, c) \\ f(a, c+h) & f(a+k, c+h) & f(a+2k, c+h) & \dots & f(b-2k, c+h) & f(b-k, c+h) & f(b, c+h) \\ f(a, c+2h) & f(a+k, c+2h) & f(a+2k, c+2h) & \dots & f(b-2k, c+2h) & f(b-k, c+2h) & f(b, c+2h) \\ \vdots & \vdots & \vdots & \ddots & \vdots & \vdots & \vdots \\ f(a, d-2h) & f(a+k, d-2h) & f(a+2k, d-2h) & \dots & f(b-2k, d-2h) & f(b-k, d-2h) & f(b, d-2h) \\ f(a, d-h) & f(a+k, d-h) & f(a+2k, d-h) & \dots & f(b-2k, d-h) & f(b-k, d-h) & f(b, d-h) \\ f(a, d) & f(a+k, d) & f(a+2k, d) & \dots & f(b-2k, d) & f(b-k, d) & f(b, d) \end{bmatrix}$$

$$\cdot \begin{bmatrix} 1 & 4 & 2 & \dots & 2 & 4 & 1 \\ 4 & 16 & 8 & \dots & 8 & 16 & 4 \\ 2 & 8 & 4 & \dots & 4 & 8 & 2 \\ \vdots & \vdots & \vdots & \ddots & \vdots & \vdots & \vdots \\ 2 & 8 & 4 & \dots & 4 & 8 & 2 \\ 4 & 16 & 8 & \dots & 8 & 16 & 4 \\ 1 & 4 & 2 & \dots & 2 & 4 & 1 \end{bmatrix} \cdot \frac{1}{9} \cdot k \cdot h$$

For each small part of the surface,  $\Delta A$ , we look at, the position of it's centre is known, and the vector,  $\vec{r}$ , from the person to  $\Delta A$  is given by:

$$\vec{r} = \begin{bmatrix} x_p - x_{\Delta A} \\ y_p - y_{\Delta A} \\ z_p - z_{\Delta A} \end{bmatrix} = \begin{bmatrix} x_r \\ y_r \\ z_r \end{bmatrix}$$

where  $k$  is the grid size in x-direction,  $h$ , is the grid size in the y-direction.

The matrix weighting the results can be made in 5 steps:

- Step 1: Make a matrix of ones with  $N$  rows and  $M$  columns corresponding to the division of the surface, both  $N$  and  $M$  has to be even numbers.
- Step 2: Row 2  $\rightarrow (N - 1)$  is multiplied by 2
- Step 3: Column 2  $\rightarrow (M - 1)$  is multiplied by 2

- Step 4: Row 2 → (N – 1) is multiplied by 2 in every 2nd row
- Step 5: Column 2 → (N – 1) is multiplied by 2 in every 2nd column

$$\begin{bmatrix} 1 & 1 & 1 & 1 & 1 & 1 & 1 \\ 1 & 1 & 1 & 1 & 1 & 1 & 1 \\ 1 & 1 & 1 & 1 & 1 & 1 & 1 \\ 1 & 1 & 1 & 1 & 1 & 1 & 1 \\ 1 & 1 & 1 & 1 & 1 & 1 & 1 \\ 1 & 1 & 1 & 1 & 1 & 1 & 1 \\ 1 & 1 & 1 & 1 & 1 & 1 & 1 \end{bmatrix} \rightarrow \begin{bmatrix} 1 & 1 & 1 & 1 & 1 & 1 & 1 \\ 2 & 2 & 2 & 2 & 2 & 2 & 2 \\ 2 & 2 & 2 & 2 & 2 & 2 & 2 \\ 2 & 2 & 2 & 2 & 2 & 2 & 2 \\ 2 & 2 & 2 & 2 & 2 & 2 & 2 \\ 2 & 2 & 2 & 2 & 2 & 2 & 2 \\ 1 & 1 & 1 & 1 & 1 & 1 & 1 \end{bmatrix}$$

$$\rightarrow \begin{bmatrix} 1 & 2 & 2 & 2 & 2 & 2 & 1 \\ 2 & 4 & 4 & 4 & 4 & 4 & 2 \\ 2 & 4 & 4 & 4 & 4 & 4 & 2 \\ 2 & 4 & 4 & 4 & 4 & 4 & 2 \\ 2 & 4 & 4 & 4 & 4 & 4 & 2 \\ 2 & 4 & 4 & 4 & 4 & 4 & 2 \\ 1 & 2 & 2 & 2 & 2 & 2 & 1 \end{bmatrix} \rightarrow \begin{bmatrix} 1 & 2 & 2 & 2 & 2 & 2 & 1 \\ 4 & 8 & 8 & 8 & 8 & 8 & 4 \\ 2 & 4 & 4 & 4 & 4 & 4 & 2 \\ 4 & 8 & 8 & 8 & 8 & 8 & 4 \\ 2 & 4 & 4 & 4 & 4 & 4 & 2 \\ 4 & 8 & 8 & 8 & 8 & 8 & 4 \\ 1 & 2 & 2 & 2 & 2 & 2 & 1 \end{bmatrix}$$

$$\rightarrow \begin{bmatrix} 1 & 4 & 2 & 4 & 2 & 4 & 1 \\ 4 & 16 & 8 & 16 & 8 & 16 & 4 \\ 2 & 8 & 4 & 8 & 4 & 8 & 2 \\ 4 & 16 & 8 & 16 & 8 & 16 & 4 \\ 2 & 8 & 4 & 8 & 4 & 8 & 2 \\ 4 & 16 & 8 & 16 & 8 & 16 & 4 \\ 1 & 4 & 2 & 4 & 2 & 4 & 1 \end{bmatrix}$$

A.2. Surface to surface

In the calculations, the numerical solution is found by first looking at the small area ΔA<sub>1</sub> and calculating the view factor from this small area to object 2. When this has been done for all the small areas of object 1, then the total view factor can be found.

The normal vectors of the surfaces are given as:

$$\rightarrow n_1 = \begin{bmatrix} x_{n_1} \\ y_{n_1} \\ z_{n_1} \end{bmatrix} \quad \rightarrow n_2 = \begin{bmatrix} x_{n_2} \\ y_{n_2} \\ z_{n_2} \end{bmatrix}$$

For each small are of the surfaces, ΔA<sub>1</sub> and ΔA<sub>2</sub> we look at the position of the centres and can thus calculate the vector,  $\vec{r}$ , between them:

$$\vec{r} = \begin{bmatrix} x_{\Delta A_2} - x_{\Delta A_1} \\ y_{\Delta A_2} - y_{\Delta A_1} \\ z_{\Delta A_2} - z_{\Delta A_1} \end{bmatrix} = \begin{bmatrix} x_r \\ y_r \\ z_r \end{bmatrix}$$

The length of  $\vec{r}$  is:

$$r^2 = x_r^2 + y_r^2 + z_r^2$$

The angle, γ<sub>1</sub>, between the normal vector of surface 1, → n<sub>1</sub>, and the vector,  $\vec{r}$ , is:

$$\cos(\gamma_1) = \frac{\rightarrow n_1 \cdot \vec{r}}{|\rightarrow n_1| \cdot |\rightarrow r|} = \frac{\begin{bmatrix} x_{n_1} \\ y_{n_1} \\ z_{n_1} \end{bmatrix} \cdot \begin{bmatrix} x_r \\ y_r \\ z_r \end{bmatrix}}{\sqrt{x_{n_1}^2 + y_{n_1}^2 + z_{n_1}^2} \cdot \sqrt{x_r^2 + y_r^2 + z_r^2}}$$

The angle, γ<sub>2</sub>, between the normal vector of surface 2, → n<sub>2</sub>, and the vector,  $\vec{d}$ , is:

$$\cos(\gamma_2) = \frac{\rightarrow n_2 \cdot (-\vec{r})}{|\rightarrow n_2| \cdot |\rightarrow r|} = \frac{\begin{bmatrix} x_{n_2} \\ y_{n_2} \\ z_{n_2} \end{bmatrix} \cdot \begin{bmatrix} -x_r \\ -y_r \\ -z_r \end{bmatrix}}{\sqrt{x_{n_2}^2 + y_{n_2}^2 + z_{n_2}^2} \cdot \sqrt{x_r^2 + y_r^2 + z_r^2}}$$

To optimise the calculation time when solving Eq. (12) the Simpson method is used – twice.

References

- [1] P.O. Fanger, Thermal Comfort. Analysis and Applications in Environmental Engineering, Danish Technical Press, Copenhagen, 1970.
- [2] S. Olesen, P.O. Fanger, P. Jensen, O. Nielsen, Comfort Limits for Man Exposed to Asymmetric Thermal Radiation, 1973.
- [3] P.O. Fanger, G. Langkilde, B.W. Olesen, N.K. Christensen, S. Tanabe, Comfort limits for asymmetric thermal radiation, Energy Build. 8 (1985) 225–236.
- [4] M.H. Vorre, R.L. Jensen, Does variation in clothing make us more thermally comfortable? in: Indoor Air 2014, Hong Kong, 2014.
- [5] M.H. Vorre, R.L. Jensen, P.V. Nielsen, Draught risk index tool for building energy simulations, in: WSB 2014 Barcelona, Barcelona, 2014.
- [6] L. Karlsen, G. Grozman, P.K. Heiselberg, I. Bryn, Operative temperature and thermal comfort in the sun – implementation and verification of a model of IDA ICE, in: Indoor Air 2014, (July 7–12, 2014, Hong Kong), Hong Kong, 2014, p. pHP0681.
- [7] P.O. Fanger, L. Banhidi, B.W. Olesen, G. Langkilde, Comfort limits for heated ceilings ASHRAE Trans. 86 (1980) 141–156.
- [8] J.R. Breckenridge, Technical Report EP-175, Effective Area of Clothed Man for Solar Radiation, Natick, MA, 1961.
- [9] J. Hardy, E. DuBois, The technic of measuring radiation and convection, J. Nutr. 15 (1938) 461–475.
- [10] A. Guibert, C.L. Taylor, Radiation area of the human body, J. Appl. Physiol. 5 (1952) 24–37.
- [11] P. Taylor, Middle East Trials: Meteorological Observations (July–August, 1955), Clothing and Stores Exper. Establ. Report No. 67, Gt. Britain, 1956.
- [12] F.A. Chrenko, L.G.C.E. Pugh, The contribution of solar radiation to the thermal environment of man in Antarctica, Proc. R. Soc. B: Biol. Sci. (1961), p. B155: 243–265.
- [13] C.R. Underwood, E.J. Ward, The solar radiation area of man, Ergonomics 9 (1966) 155–168.
- [14] P.O. Fanger, O. Angelius, P. Kjerulf-Jensen, Radiation data for the human body, ASHRAE Trans. (1970) 338–373.
- [15] M. Steinman, L. Kalisperis, L. Summers, Angle factor determination from a person to inclined surfaces, ASHRAE Trans. 94 (1988) 1809–1823.
- [16] T. Horikoshi, T. Tsuchikawa, Y. Kobayashi, E. Miwa, Y. Kurazumi, K. Hirayama, The effective radiation area and angle factor between man and a rectangular plane near him, ASHRAE Trans. 96 (1) (1990) 60–66.
- [17] G. Rizzo, G. Franzitta, G. Cannistraro, Algorithms for the calculation of the mean projected area factors of seated and standing persons, Energy Build. 17 (1991).
- [18] G. Cannistraro, G. Franzitta, C. Giaconia, G. Rizzo, Algorithms for the calculation of the view factors between human body and rectangular surfaces in parallelepiped environments, Energy Build. 19 (1992) 51–60.
- [19] A. Nucara, M. Pietrafesa, G. Rizzo, Computing view factors between human body and non parallelepiped enclosures, Proc. Healthy Build. 2 (2000) 611–616.
- [20] M. La Gennusa, A. Nucara, M. Pietrafesa, G. Rizzo, G. Scaccianocce, Angle factors and projected area factors for comfort analysis of subjects in complex confined enclosures: analytical relations and experimental results, Indoor Built Environ. 17 (2008) 346–360.
- [21] G. Walton, Calculation of Obstructed View Factors by Adaptive Integration, Gaithersburg, USA, 2002.
- [22] European Committee for Standardization, EN ISO 7730 (2006).